

# A Basic Lattice Model of an Excitable Medium: Kinetic Monte Carlo Simulations

A. G. Makeev\* and N. L. Semendyaeva\*\*

*Moscow State University, Moscow, Russia*

\*e-mail: amak@cs.msu.ru;

\*\*e-mail: natalys@cs.msu.ru

Received August 10, 2015

**Abstract**—The simplest stochastic lattice model of an excitable medium is considered. Each lattice cell can be in one of three states: excited, refractory, or quiescent. Transitions between different cell states occur with the prescribed probabilities. The model is designed for studying the transfer of excitation in the cardiac muscle and nerve fiber at the cellular and subcellular levels, and also for modeling the spreading of epidemics. Elementary events on the lattice are simulated by the kinetic Monte Carlo method, which consists in constructing a Markov chain of the lattice states corresponding to the solution of the master equation. An effective algorithm for implementing the Kinetic Monte Carlo simulations is suggested. The number of the arithmetic operations at each time step of the proposed algorithm is practically independent of the lattice size, which enables making calculations on two- and three-dimensional lattices of a very large size (more than  $10^9$  cells). It is shown that the model reproduces the basic space-time structures (solitary running pulses, pulse strings, concentric and spiral waves, and spiral turbulence) characteristic of an excitable medium. The basic properties of traveling pulses and spiral waves for the considered stochastic lattice model are studied and compared with the known properties of deterministic equations of the reaction-diffusion type, which are usually employed for modeling excitable media.

**Keywords:** excitable media, traveling pulses, spiral waves, lattice models, Kinetic Monte Carlo simulations

**DOI:** 10.1134/S2070048217050088

## 1. INTRODUCTION

The article published in 1946 [1] is the seminal work on the mathematical modeling of spatial structures in an excitable medium. In this publication, the mathematician, Norbert Wiener, who is also considered the founder of cybernetics, and the cardiologist, Arturo Rosenblueth, formulated the basic principles of the mathematical description of transmitting excitation in the cardiac muscle and nerve fiber. The authors' model assumes that each cell can be in one of three states, i.e., excited, refractory, or quiescent. An excited cell can either transfer excitation to the neighboring cells if they are quiescent or pass to the refractory state, in which the cell becomes temporarily resistant to excitation but then passes to the quiescent state. Wiener and Rosenblueth showed the possible emergence of plane excitation waves and spiral waves in a system of interacting myocardial cells and also discussed the possible role of spiral waves in the appearance of pathological conditions of the heart, such as flutter and ventricular fibrillation.

In addition to the cardiac muscle, other bright examples of an excitable medium include reactions on the surface of the catalyst, the Belousov–Zhabotinsky reaction, a forest fire, and a wave of greetings among football fans at a stadium (the Mexican wave). Despite the different physical meanings of these phenomena, they all exhibit similar properties that are characteristic of excitable media.

Since the 1970s, spatial structures in excitable media have been mathematically modeled mainly with the help of deterministic nonlinear partial differential equations of the reaction-diffusion type [2–4]. For such equations, the classical model of an excitable medium is characterized by the fact that it has a single quiescent state that is stable with respect to small perturbations. Alongside this, a sufficiently strong perturbation can excite a travelling wave in such a medium, after passing through which the system returns to the original quiescent state. The main driving force for the traveling wave is the diffusion process through which excitation is transferred over space.

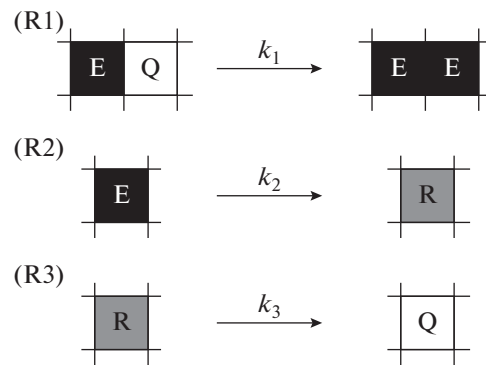


**Fig. 1.** Possible elementary events on lattice. Each cell can be in one of three following states: excited (“E”), refractory (“R”), or quiescent (“Q”).

The mathematical model proposed in [1] can be called the basic axiomatic model of an excitable medium. There are several options for its specific implementation; for example, this can be done with the help of cellular automata [5]. In this paper, modeling is carried out by Kinetic Monte Carlo simulations (Kinetic Monte Carlo, KMC [6, 7]). The system of interacting cells is represented in the form of cells of a square lattice. The three possible states of each cell are excited, refractory, and quiescent. On the lattice, three possible variants of elementary events (reactions (R1)–(R3)) are considered, which can occur with transition probabilities  $k_1$ ,  $k_2$ , and  $k_3$  [ $\text{sec}^{-1}$ ], respectively, as shown in Fig. 1. It is assumed that the evolution of this system obeys the basic kinetic equation (master equation) describing the time variation in the observation probability of a particular lattice state for a discrete set of states. The events on the lattice are simulated by the KMC method, which consists in constructing a Markov chain of the lattice states corresponding to the solution of the master equation. Unlike modeling based on cellular automata where changes in the lattice state are subject to rather arbitrarily introduced rules, calculations using the KMC method operate with transition probabilities that have a simple and understandable physical meaning.

The mathematical model considered here had been studied earlier by other authors; however, they presented it as a lattice-based susceptible-infected-recovered-susceptible (SIRS) epidemic model [4, 8]. In this case, the population is represented as cells of a square lattice. There are three possible states of each cell: those that have been infected with the disease and are capable of spreading it further (Infected), those that have recovered with temporary immunity (Recovered), and those that have not yet been infected but which can be infected from neighboring infected individuals (Susceptible). The SIRS model is completely equivalent (within the notation) to the reaction model (R1)–(R3) considered in this paper. The lattice-based SIRS model has been studied using the Monte Carlo method, for example, in [8], but it has not conceptually been considered as a typical model of an excitable medium.

In this paper, the following problems are solved: (1) an effective algorithm has been developed for calculating the KMC reaction model (R1)–(R3) on large two-dimensional square and three-dimensional cubic lattices of more than  $10^9$  cells; (2) it has been shown that this model reproduces the main space-time structures typical of an excitable medium; (3) the primary properties of traveling pulses and spiral waves have been studied.

## 2. KINETIC MONTE CARLO SIMULATIONS

The algorithm for simulating the reaction process on a lattice using the KMC kinetic method consists of the following steps [6, 7].

*I. Setting the initial state of the lattice.*

*II. Calculating the velocities of the elementary events.* At the current time, the velocities of all possible elementary events, which transfer the lattice to a new state, are calculated; this is followed by the calculation of the total velocity  $R$ .

*III. Selecting an event and changing the state of the lattice.* One of the possible elementary events is randomly chosen with the probability of its occurrence proportional to its velocity. The lattice state is changed according to the selected event

IV. *Calculation of the time step.* The time  $t_2$  of the system's exit from the current state is calculated:  $t_2 = t_1 - (\ln(\xi)/R)$  where  $\xi$  is a random quantity uniformly distributed over the interval  $(0, 1)$ . The transition to the next step to stage II is carried out if the specified maximum time value is not reached.

This algorithm is a rejection-free variant of the KMC method [9, 10] because one elementary event necessarily occurs at each time step. There are also other varieties of the KMC method, for example, the rejection KMC algorithm. Different variants of the KMC method are statistically equivalent but their effectiveness depends on the specifics of the studied problem. In particular, the rejection algorithm becomes inefficient if the velocities of the elementary events significantly differ from each other, i.e., when the studied system is characterized by rigidity [10]. Therefore, the rejection-free KMC method is more comprehensive.

Normally, it is sufficient to calculate the velocities of all possible elementary acts (stage II) only at the initial time, and then to calculate only those velocities that have changed as a result of the occurrence of the selected elementary event. In other words, the procedure can be confined to the local recalculation of the velocities at each time step, which will significantly reduce the computational costs. The most time-consuming calculation is at the stage of selecting a single event (stage III). Now we consider possible options for organizing this choice.

### 2.1. Algorithm 1 (Linear Search)

For the current configuration, let the variables  $r_j$ , where  $j = 1, \dots, M$ , denote the velocities of the possible elementary events changing the state of the lattice. The total velocity of the change in the current state of the lattice  $R$  is  $\sum_{j=1}^M r_j$ . At each time step, a random choice must be made from all velocities  $r_j$  to select one with the number  $p$  with the probability  $r_p/R$ . This requires a random real number  $\xi \in (0, 1)$  and the number  $p$  is determined such that  $\sum_{j=1}^{p-1} r_j < \xi R \leq \sum_{j=1}^p r_j$ . Such a choice of one elementary event is called a linear search.

The velocities'  $r_j$  being not ordered necessitates a simple linear search. At each step of the linear search, two operations with real numbers are performed, i.e., addition and comparison. If all the events are assumed to be equally probable, the choice of a single event will require on average  $M$  floating-point operations. The value of  $M$  can be taken to be proportional to the number of nodes (cells)  $N$  of the lattice. Therefore, on a lattice with a large number of nodes, a linear search becomes practically unsuitable because of the large computational costs. The advantages of this approach are the simplicity of its software implementation and minimal use of RAM. There are various approaches to significantly reduce the number of arithmetic operations required for the selection of one event at each time step of the KMC method. Here is a general description of the most effective algorithm for selecting an elementary event on a large-size lattice.

### 2.2. Algorithm 2

It is necessary to identify in advance all the possible total velocities of the change in the state of a single cell. This means not only a numerical coincidence between the sum of the velocities of possible events but also a complete coincidence between the list of elementary events themselves. Various total velocities are denoted by  $R_k$ , where  $k = 1, \dots, m$ ;  $m$  is the general number of various total velocities for one cell. Each value  $R_k$  is the sum of one or several velocities of elementary events  $r_j$ . Let the total number of summands in  $R_k$  be  $m_k$ . It should be noted that some (two-node) lattices can yield several summands in the calculation of  $R_k$ . The values  $R_k$ ,  $m$ , and  $m_k$  are determined in advance; they do not change in the process of computation. Besides, the values  $m$  and  $m_k$  do not depend on the number of the lattice nodes  $N$ .

The numbers of lattice nodes, for which the total velocities of the change in their state are similar and equal to  $R_k$ , are stored in separate integer arrays  $A_k$ . Let  $N_{A_k}$  ( $0 \leq N_{A_k} \leq N$ ) be the number of elements in the array  $A_k$ . The values  $N_{A_k}$  and  $A_k[j]$ , where  $j = 1, \dots, N_{A_k}$ , change in the course of the computation depending on the state of the lattice. The total velocity of the change in the state of the entire lattice is  $\sum_{k=1}^m (N_{A_k} R_k)$ .

The choice of one elementary event is made in three stages.

(1) Using a random real number  $\xi \in (0, 1)$ , we select the number  $k$  of one of the arrays  $A_k$  ( $k = 1, \dots, m$ ) by a linear search through the summands of the form  $N_{A_k} R_k$ , contributing to the total velocity  $R$ .

(2) A random integer  $\xi_{\text{int}} \in [1, N_{A_k}]$  is generated with a uniform distribution and the number of one node  $i_* = A_k[\xi_{\text{int}}]$  is selected.

(3) If the total velocity  $R_k$  includes several elementary events, then one of these is selected by the linear search through  $m_k$  events. To this end, another random integer  $\xi_1 \in (0, 1)$  is generated.

After selecting one elementary event, the lattice state should be changed and the velocities of the elementary events of the lattice change should be locally recalculated. Moreover, the velocities at the node  $i_*$  and in its vicinity must be recalculated and one or more values of  $N_{A_k}$  and  $A_k[j]$  must be changed in accordance with the local change in the lattice state. The total velocities  $R_k$  can be changed not only for the nodes with the changed states but also for the neighboring nodes. Since the node numbers in the arrays  $A_k$  are not ordered, it is required also to store the change during the calculation in a table, which for each node makes a reference to the respective number  $k$  and to the location of the number of this node in the array  $A_k$ . A more detailed consideration of Algorithm 2 is given in the next section and illustrated by the following example.

### 2.3. Comparison of the Algorithms' Efficiency

The main advantage of Algorithm 2 is that the number of arithmetic operations at each time step is practically independent of the number of lattice nodes  $N$ . Stage 2 of Algorithm 2 does not include a sequential search for an elementary event but involves the random selection of one of equally probable events. The linear search (Algorithm 1) requires about  $O(M)$  floating-point operations at every step; at the same time, the value of  $M$  changes in the course of the calculation but it can be considered approximately equal to the number of nodes  $N$ . Algorithm 2 requires about  $O(2m + m_k)$  operations at every step, where the values  $m$  and  $m_k$  are known in advance and as a rule they are much smaller than  $N$ . When the reactions are rather simple, the characteristic values of the sum  $2m + m_k$  can be taken as 10–20. The fact that the choice of one process in Algorithm 2 requires the generation of two or three random numbers, whereas in Algorithm 1, only one random number has to be used is not material. The generation of one pseudorandom integer is performed by fast integer operations, which correspond to  $\approx 4$  floating-point operations (the real pseudorandom number is obtained from the integer by one additional division operation).

The construction of the most effective algorithm for selecting an elementary event in the KMC-based calculations depends on the specific nature of the problem. For the problem considered below, on a lattice with  $N = 10^8$  nodes, Algorithm 1 would require the computation time to be longer by a factor of about  $10^6$  than Algorithm 2. An algorithm for the choice of one elementary event analogous to Algorithm 2 is described in [9]. The main ideas of this approach are based on work [6] (the algorithm “n-fold way”) where the KMC method was used for the Ising lattice model. In another fundamental work using the KMC method [7], a simple linear search was used even though such an algorithmic approach was justified since reactions were considered in well-mixed systems, for which  $N = 1$ , and the number  $M$  is small and denotes the number of different chemical reactions. Another popular algorithm for choosing one elementary event is *binary search* [9, 10]; this algorithm requires about  $O(\log_2(M))$  floating-point operations at every time step. However, for a large lattice Algorithm 2 will be more effective than a binary search if the number of different total velocities for one node is not very large. When implementing a binary search, the whole set of different velocities is divided into subsets and partial sums are computed (the sums of the velocities for the subsets). In evaluating the effectiveness of a particular variant of the KMC method, the costs required for the preparation for a new time step should also be taken into account. After the occurrence of one elementary event, it is required not only to recalculate some local velocities but also to introduce changes to the data structures used to select an elementary event. In this case, Algorithm 2, in contrast to the binary search, does not require any additional calculations of the partial sums; only memory operations are necessary, while floating-point calculations are not used.

### 3. THE SIMPLEST LATTICE MODEL OF AN EXCITABLE MEDIUM

We consider a two-dimensional square  $N = N_1 \times N_2$  lattice with periodic boundary conditions or with boundary conditions of the free boundary type. Each cell (mesh) with the number  $i$ , where  $i = 1, \dots, N$ , can be in one of the three states {"E," "R," or "Q"}. Let  $N_E$ ,  $N_R$ , and  $N_Q$  be the total number of cells in the state "E," "R," and "Q," respectively. The concentrations of the different states are denoted by  $u$ ,  $v$ , and  $w$ :  $u = N_E/N$ ;  $v = N_R/N$ ; and  $w = N_Q/N = 1 - u - v$ . On the lattice, we consider three possible variants of elementary events (reactions) that can occur with transition probabilities  $k_1$ ,  $k_2$ , and  $k_3$  [ $\text{sec}^{-1}$ ], respectively (see Fig. 1).

- (R1) An excited cell sends excitation to a neighboring cell if the latter is in a quiescent state ( $E + Q \rightarrow E + E$ ). On a square lattice, each cell has four adjacent cells (in Fig. 1 only one cell is shown).
- (R2) An excited cell passes to the refractory state ( $E \rightarrow R$ ).
- (R3) A refractory cell passes to the quiescent state ( $R \rightarrow Q$ ).

In order to apply the KMC method and Algorithm 2 to the model (R1)–(R3), all possible total velocities of the change in the condition of one cell must be identified in advance. If a cell is in the state "R," the velocity of the change in its state is  $k_3$ , regardless of the state of the adjacent of its adjacent environment. If a cell is in the state "Q," then the velocity of a change in its state is formally considered equal to 0 because the elementary event (R1) is taken into account for the "E" type cells. If a cell with the number  $i$  is in the state "E" then the total velocity of the change in its state,  $R_{E,k}$ , can assume one of five values, i.e.,  $R_{E,k} = k_2 + k_1 k$ , where  $k = 0, \dots, 4$  is the number of adjacent cells for the cell with the number  $i$  in the state "Q." The total velocity  $R_{E,k}$  includes the velocities at which events (R1) and (R2) occurred. Let the one-dimensional integer arrays  $A_k$  contain the numbers of cells and let the total velocity of each one be  $R_{E,k}$ . Let  $N_{A_k}$  be the current number of elements in the array  $A_k$  ( $k = 0, \dots, 4$ ). The values  $N_{A_k}$  and  $A_k[j]$ , where  $j = 1, \dots, N_{A_k}$ , change in the course of the calculation depending on the state of the lattice.

For the KMC simulation of the events (R1)–(R3), in the time interval  $t = [0, t_{\max}]$ , the following sequence of actions is performed at each time step.

1. The values  $r_1 = k_3 N_R$  and  $r_{k+2} = N_{A_k} R_{E,k}$  ( $k = 0, \dots, 4$ ) and the total velocity  $R = \sum_{j=1}^6 r_j$  are calculated at the current time  $t_1 = t$ .
2. A single value  $r_j$  ( $j = 1, \dots, 6$ ) is randomly selected using a linear search. To this end, a random real number  $\xi \in (0, R)$  is generated.
3. If the value  $r_1$  is chosen, any cell of type "R" must be found. To do this, random numbers of cells  $i_1 = \xi_{\text{int}}$ , where  $\xi_{\text{int}} \in [1, N]$ , are generated until such a cell has been found. Then the event (R3) occurs and the state of the obtained cell  $i_1$  is changed to "Q." The transition to stage 5 is implemented.
4. If at stage 2 the value  $r_j$  is selected, where  $j = 2, \dots, 6$ , a random integer is generated  $\xi_{\text{int}} \in [1, N_{A_{j-2}}]$  and the number of one cell  $i_1 = A_{j-2}[\xi_{\text{int}}]$  is defined. If  $j = 2$ , then in the cell  $i_1$  the event (R2) occurs and the transition to stage 5 is implemented. At  $j > 2$ , a new random real integer  $\xi_1 \in (0, 1)$  is generated and if  $\xi_1 \leq k_2/(k_2 + k_1(j-2))$  the event (R2) occurs in the cell  $i_1$ . Otherwise, the event (R1) is realized in the cell  $i_1$  and one of its neighboring cells. In order to choose  $i_2$  at  $j > 3$ , a random integer from the range  $[1, j-2]$  is used.
5. Depending on the realized elementary event, the values  $N_E$ ,  $N_R$ , and  $N_Q$  change to  $\pm 1$ . Cells  $i_1$  and  $i_2$  are locally recalculated ( $i_2$  only in the case of the event (R1)), as well as for the environment nearest to them; to do this, appropriate changes are made to the values  $N_{A_k}$  and  $A_k$ .
6. A new time instant is calculated:  $t = t_1 - (\ln(\xi_t)/R)$ , where  $\xi_t \in (0, 1)$ . The transition to the next step to stage 1 is implemented if  $t \leq t_{\max}$ .

Additional comments should be made to the organization of a local recalculation. In order to remove the specified cell number from the array  $A_k$ , its sequence number in the array must be known. Cell numbers in the arrays  $A_k$  are not ordered; therefore, an additional two-dimensional integer array  $H[p, i]$  (where  $p = 1, 2$ ;  $i = 1, \dots, N$ ), which contains the number  $k = H[1, i]$  of the required array  $A_k$  and the sequence

number  $H[2, i]$  of the required value  $i$  in the array  $A_k$ , should be stored. By definition,  $A_{H[1, i]}[H[2, i]] = i$ . If during the recalculation the number of elements  $N_{A_k}$  in the array  $A_k$  increases, a new element is added to the end of the array; if some element has to be removed, an element from the end of the array is put into its place.

At stage 3 of the algorithm, a cell of type “R” is randomly selected; in this case, the numbers of such cells are not stored in an additional array  $A_k$  as they are for cells of type “E.” The cell for an elementary event (R3) is chosen by randomly searching the entire lattice rather than using the approach employed in Algorithm 2. In the calculations discussed in this paper, the concentration is usually  $> 0.5$ ; therefore, on average no more than two random integers will have to be generated to find the necessary cell. The random search for a cell of type “R” makes it possible to reduce computational costs (both computing time and RAM resources).

The calculations used a 64-bit version of the pseudorandom number generator Mersenne Twister. In order to obtain the random integer  $\xi_{\text{int}} \in [1, n]$ , the random integer  $\xi_* \in [0, 2^{64} - 1]$  was generated and the value  $\xi_{\text{int}} = (\xi_* \bmod n) + 1$  was calculated, where  $\bmod$  denotes the operation of calculating the remainder in the integer division. Under  $(2^{64} \bmod n) \neq 0$ , only such values  $\xi_*$  were used for which the inequality  $\xi_* < 2^{64} - (2^{64} \bmod n)$  is satisfied.

The algorithm is designed in such a way that the number of arithmetic operations at every time step is practically independent of the number of cells  $N$ . The procedure for selecting one elementary event requires on average only about 10 floating-point operations. It should be noted that usually much fewer arithmetic operations for a linear search are required in stage 2 than for a linear search through equiprobable values, because the values  $r_j$  differ greatly and they are automatically in descending order. The time required for the local recalculation is about 30% of the total duration of the calculation, and the costs for generating pseudorandom integers are less than 10% of the total cost. The proposed algorithm can easily be generalized to the case of other two-dimensional lattices (rectangular and hexagonal), and also to the three-dimensional case.

#### 4. CALCULATION RESULTS

The program we developed makes it possible to perform calculations on a lattice containing up to  $4 \times 10^9$  cells on a computer with 32 Gb of RAM. The calculations were carried out on two-dimensional square and three-dimensional cubic lattices. Let us consider basic space-time structures arising in the KMC calculation of the reaction model (R1)–(R3).

Figure 2 shows a typical plane excitation wave, which can be observed in calculations using the KMC method if the appropriate initial distribution is specified. The wave (pulse) moves from left to right. The calculations were performed on a  $400 \times 1000$  lattice with periodic boundary conditions. Here and below, cells of type “E” are shown in black, cells of type “R” are shown in gray, and type “Q” cells are shown in white. At the initial moment, all the cells except for the five extreme left columns of the lattice were in the quiescent state (white background); the cells in the four extreme left columns were specified as being in the “R” state, and the fifth column consisted of excited cells. Figure 2 shows the generated traveling pulse. The leading edge of the pulse consists mainly of cells in the excited state. As the pulse progresses, the cells from the quiescent state first pass to the excited state, then to the refractory state, after which they return to the quiescent state. The leading edge (head) of the pulse is constantly changing (fluctuating) but no qualitative change in its structure is observed. For a stochastic model, such a traveling pulse is called *plane*, although it is not ideally plane because of the fluctuations. Since periodic boundary conditions are imposed, the traveling pulse does not disappear and can be observed to be arbitrarily long; however, because of the insufficiently large horizontal size of the lattice  $N_2$ , its head and tail interact with each other (Fig. 2c). In this case, the leading edge of the pulse propagates against the background of the cells, some of which are already in the refractory state. The tail of the pulse consists of cells of types “R” and “Q,” and the local concentration of the cells of type “R” gradually decreases as the distance from the head of the pulse increases. For large values of  $N_2$ , a solitary pulse would be observed. A similar plane traveling pulse can be excited in a three-dimensional model.

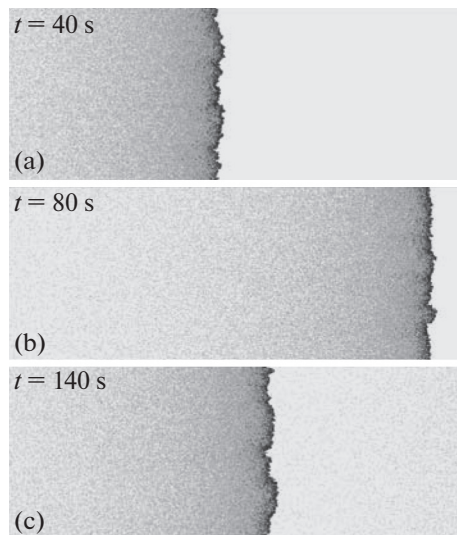


**Fig. 2.** Plane excitation waves on lattice sized  $400 \times 1000$  with periodic boundary conditions. Values of the parameters:  $k_1 = 5$ ,  $k_2 = 1$ ,  $k_3 = 0.04$ . Excited cells are shown in black, refractor cells are shown in gray, and quiescent cells in white. State of cell is shown for (a)  $t = 40$  sec; (b)  $t = 80$  sec; (c)  $t = 140$  sec.

The solution in the form of a traveling pulse only exists in a limited range of values of the three model parameters when the following inequalities are satisfied:  $k_1 > k_2 \gg k_3$ . Without loss of generality, we can assume that  $k_2 = 1$  (this condition can always be obtained by normalization). For a two-dimensional lattice,  $k_1 \approx 1.5$  is the minimum value at which a traveling pulse can be observed.

At small values of  $k_1$ , the leading edge of the pulse contains only a few excited cells as can be seen from Fig. 3a for  $k_1 = 2$ . Despite this, the traveling pulse does not disappear but continues its periodic motion along the lattice (periodic boundary conditions are imposed). As  $k_1$  increases (Fig. 3b for  $k_1 = 20$ ), the head of the pulse shows an increase in the number of excited cells, while the characteristic dimensions and the velocity of the pulse also rise.

In order to characterize the *spatial* profile of a traveling pulse, the average concentration of cells of types “E” and “R” in each column  $j$  ( $j = 1, \dots, N_2$ ) of the lattice may be calculated; these concentrations are denoted by  $u_j$  and  $v_j$ , respectively. Averaging is carried out over  $N_1$  cells. Figure 4 shows the results of the calculations on a  $5000 \times 20000$  lattice with periodic boundary conditions. Because of the uneven leading edge of the pulse, the concentration  $u_j$  is always much less than 1. Nonzero values of  $u_j$  are only obtained in the head of the pulse. The tail of the pulse consists of nonzero values of  $v_j$ , which gradually decline with as  $j$  decreases.

Similar spatial dependences of the variables are observed in the calculation of partial differential equations of the activator-inhibitor type with diffusion, in particular, in the calculations of the well-known FitzHugh–Nagumo model. In our case, the role of the activator is performed by excited cells of type “E”, and the role of the inhibitor is played by the “R”-type cells. It should be noted that the lattice model of reactions (R1)–(R3) does not contain a diffusion process in the explicit form. Since the neighboring cells can transfer excitation to each other, the role of diffusion is performed by the reaction (R1). It is known that the velocity of a solitary pulse in models of the activator-inhibitor type is proportional to the value  $\sqrt{D}$ , where  $D$  is the diffusion coefficient of the activator. For the lattice model, it is of interest to study the dependence of the pulse velocity on the values of the parameter  $k_1$ .

On making stochastic calculations to find the location of a plane solitary pulse on the lattice for each row  $i = 1, \dots, N_1$ , it is possible to calculate the position of the rightmost cell of type “E” or “R,” and then calculate the mean value  $\bar{h}(t) = \frac{1}{N_1} \sum_{i=1}^{N_1} h_i(t)$ . The quantity  $\bar{h}(t)$  increases with time almost linearly, which makes it possible to determine the average pulse propagation velocity  $c_w$ , which is measured in units of cells per second. The calculations in Fig. 5 show that for the pulse velocity at rather large values of  $k_1$ , the

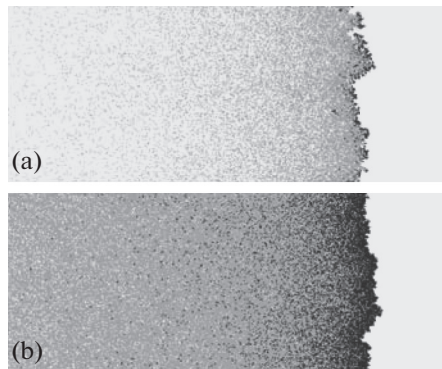


**Fig. 3.** Traveling pulses on  $200 \times 500$  lattice at  $k_2 = 1$ ,  $k_3 = 0.04$ , and various values of  $k_1$ : (a)  $k_1 = 2$ ,  $t = 100$  sec; (b)  $k_1 = 20$ ,  $t = 8$  sec.

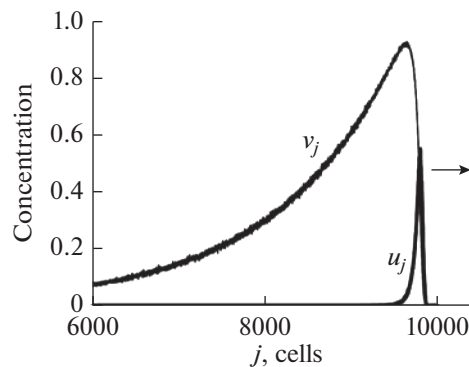


**Fig. 4.** Spatial profile of traveling (from left to right) pulse at  $k_1 = 20$ ,  $k_2 = 1$ , and  $k_3 = 0.035$ . Dependences of concentrations  $u_j$  and  $v_j$  on number  $j$  of column of  $5000 \times 20000$  lattice.

relation  $c_w \approx ak_1$  is satisfied, where  $a \approx 2.5$  for a two-dimensional lattice and  $a \approx 3.9$  for a three-dimensional lattice. Thus, we observe a near-linear dependence of the velocity  $c_w$  on the value  $k_1$ . The exact value of the proportionality coefficient  $a$  depends on the model parameters. At small values of  $k_1$ , the coefficient  $a$  is lower than the one presented above. For example, at  $k_1 = 2$ ,  $a \approx 1.955$  (for a two-dimensional square lattice). At large values of  $k_1$ , the coefficient  $a$  increases. For example, at  $k_1 = 20$ ,  $a \approx 2.467$  and at  $k_1 = 500$ ,  $a \approx 2.51$ . For a three-dimensional lattice, the pulse velocity increases compared to the two-dimensional case since for each excited cell the number of adjacent cells that can be in the quiescent state increases.

The space-time structures typical of an excitable medium in a one-dimensional case are solitary pulses and strings of pulses. One of the important characteristics of a pulse string is the so-called dispersion ratio, defined as the dependence of the propagation velocity of a pulse string  $c_w$  on the distance between consecutive pulses  $\lambda_w$  (wavelength). The dependence  $c_w(\lambda_w)$  for two values of  $k_3$  is shown in Fig. 6; it corresponds to the normal dispersion relation, which is typical of one-dimensional equations of the reaction-diffusion type. In order to construct the dependence, we considered the solution in the form of a single pulse (as in Fig. 2), albeit, with variable horizontal dimension of the lattice  $N_2$ . Since periodic boundary conditions were used, it can be assumed that  $\lambda_w = N_2$ . If the value  $N_2$  is too small, the pulse becomes unstable and disappears. If the value  $N_2$  is sufficiently large, the velocity  $c_w$  is practically independent of  $N_2$  and corresponds to the velocity of a solitary pulse. It is obvious from Fig. 6 that the velocity of a solitary pulse is practically independent of the value of  $k_3$ ; it only depends on the value of  $k_1$ . The parameter  $k_3$  determines the velocity at which the excitable medium is restored (moves to the quiescent state) after the wave has passed.



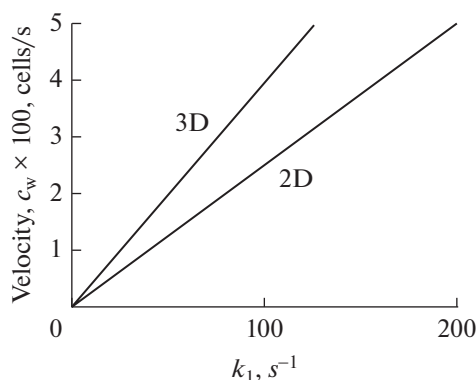


**Fig. 5.** Dependence of mean velocity of solitary traveling pulse on  $k_1$  at  $k_2 = 1$  and  $k_3 = 0.035$ . Results of calculations are shown carried out on two-dimensional (2D) and three-dimensional (3D) lattices.

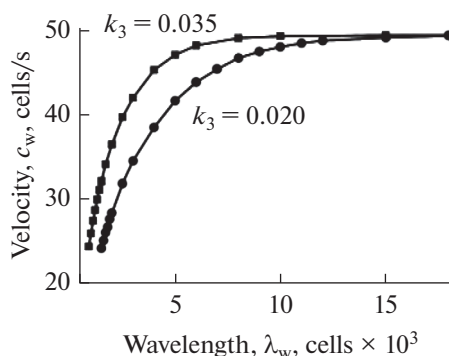


**Fig. 6.** Dependence of mean velocity of traveling pulse on wavelength for pulse string. Values of parameters:  $k_1 = 20$ ,  $k_2 = 1$ ,  $k_3 = 0.035$ , or  $k_3 = 0.02$ .

The KMC calculations have shown that traveling pulses in the lattice model have all the basic properties known from the reaction-diffusion type equations. This, in particular, is the property of annihilation under the collision of two pulses moving towards each other. Another characteristic property is the dependence of the pulse velocity on the curvature of the leading edge: if the convex (concave) leading edge of the pulse is set, its velocity will be slower (faster) than the velocity of the plane pulse.

Concentric and spiral waves are well-known space-time structures for a two-dimensional excitable medium. Such structures can also be observed in the considered lattice model when the calculations are based on the KMC method. In order to excite a concentric wave in a system, in which all cells are in the quiescent state, it is usually enough to bring one cell into an excited state. However, when the wave reaches the boundaries of the lattice, it will disappear and the system will return to the original quiescent state. A spiral wave can be obtained by setting special initial conditions (Fig. 7). The calculations were carried out on a  $10^4 \times 10^4$  lattice with boundary conditions of the free boundary type. At the initial time, in the middle of the lattice, a rectangular  $5 \times (N_2/2)$  fragment was specified, which consisted of four half-rows ( $N_2/2$ -long) cells of type “R” and one half-row of “E” cells. The remaining cells were in the quiescent state (white background). Snapshot 1 shows the starting generation of the spiral wave. After a while, a large spiral wave is formed (Snapshot 3). Then a spontaneous discontinuity is formed at one point of the leading edge (Snapshot 4). Gradually, a large spiral wave is destroyed and new fragments (scraps) of spiral waves are formed: they rotate, collide, and are partially annihilated creating new scraps. The state of the system shown in snapshots 8 and 9 is usually called spiral turbulence or spiral chaos in an excitable medium. It can arise in deterministic systems of the reaction-diffusion type due to various kinds of instabilities in solutions in the form of spiral waves [11–14] or can be caused by the presence of strong fluctuations in stochastic reaction-diffusion systems [14]. With regard to excitation waves in the cardiac muscle, this condition is also referred to as electric turbulence [12, 15], which is commonly believed to correspond to a deadly heart condition, ventricular fibrillation, which is the main cause of death for most people.

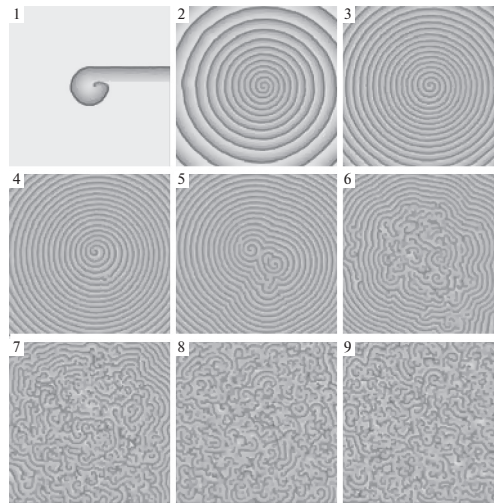


**Fig. 7.** Formation of a spiral wave and spiral chaos on  $10^4 \times 10^4$  lattice. Values of parameters:  $k_1 = 10$ ,  $k_2 = 1$ ,  $k_3 = 0.04$ . Instant snapshots of lattice state are shown at time instants  $t$ , sec: (1) 50; (2) 500; (3)  $10^3$ ; (4)  $1.5 \times 10^3$ ; (5)  $5 \times 10^3$ ; (6)  $1.5 \times 10^4$ ; (7)  $2.5 \times 10^4$ ; (8)  $3.5 \times 10^4$ ; (9)  $5 \times 10^4$ .

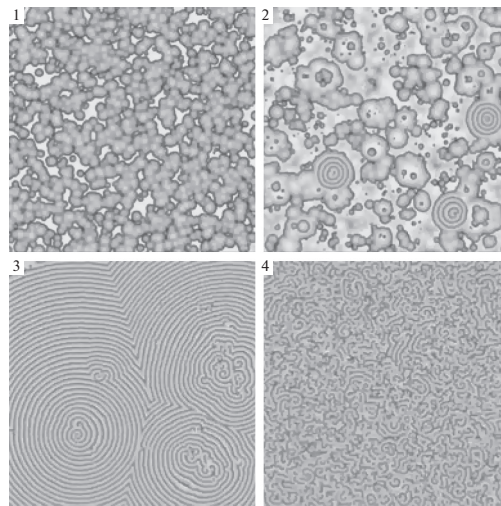


**Fig. 8.** Spontaneous formation of spiral and concentric waves, followed by generation of spiral chaos on lattice  $20000 \times 20000$  at  $k_1 = 20$ ,  $k_2 = 1$ ,  $k_3 = 0.06$ . At initial instant of time, random initial distribution is specified for  $u = 10^{-4}$ ,  $v = 0.6$ . Instant snapshots of lattice state are shown at time instants  $t$ , sec: (1) 50; (2) 500; (3) 3300; (4)  $2.5 \times 10^4$ .

For the lattice model under study, the state of spiral turbulence can continue for an arbitrarily long time period. In some cases, a large spiral wave makes 100 or more rotations before an accidental edge discontinuity occurs; this break is observed near the tip of the spiral wave. A similar scenario for the formation of spiral turbulence was described in [16] for the Lattice Lotka–Volterra (LLV model). It should be noted that the model we are considering contains a simpler set of reactions than the LLV model. In both cases, three states of each lattice cell are singled out; however, for the LLV model, the reaction (R2) should be written in the form  $R + E \rightarrow R + R$  (reactions (R1) and (R3) remain the same). In this case, for a cell passing from the excited state to the refractory state, the presence of an adjacent refractory cell is required, which is a complication of the reaction (R2).

For the stochastic model under study, the spontaneous generation of spiral and concentric waves is possible in the absence of inhomogeneities in the system; an example of such calculations is presented in Fig. 8. Here a random initial distribution was specified for  $u = 10^{-4}$ ,  $v = 0.6$ . In a short time ( $t = 50$  sec,

Snapshot 1), many small concentric waves were generated in the system. This was followed by a spontaneous generation of several fragments of spiral waves ( $t = 500$  sec, Snapshot 2), which generate large periodic concentric waves; over time they occupy the entire lattice ( $t = 3300$  sec, Snapshot 3). This is followed by a gradual destruction of large concentric waves and after a comparatively long time spiral turbulence is formed ( $t = 2.5 \times 10^4$  sec, Snapshot 4). Hereinafter, this state does not change qualitatively.

## 5. DETERMINISTIC MODELS OF REACTIONS (R1)–(R3)

At the microlevel, the initial problem is determined by specifying the lattice model and the kinetic scheme of the reactions; and the probabilities of the transitions between the different possible lattice cell states are the parameters of the model. The KMC method provides an exact solution to the problem but it involves large computational costs. To describe the behavior of the system at the meso- and macrolevels, deterministic models are usually used, which are derived from the master equation under certain assumptions and, therefore, yield only an approximate solution of the original problem.

Let the elementary events (R1)–(R3) occur on an infinite square lattice. Suppose that there are no spatial correlations between the values of the states of the lattice cell. In other words, at any instant of time the states of the cells' occupancy are randomly distributed at the specified state concentrations  $u$  and  $v$ . Then the variation of values  $u$  and  $v$  with time is described by the following system of ordinary differential equations (ODEs):

$$\begin{cases} du/dt = 4k_1u(1-u-v) - k_2u = f_1, \\ dv/dt = k_2u - k_3v = f_2. \end{cases} \quad (1)$$

System (1) always has a trivial stationary solution ( $u = 0, v = 0$ ). This solution corresponds to the state of the lattice where all the cells are in the quiescent state. There also exists a nontrivial stationary solution ( $u_*, v_*$ ), calculated from formulas  $u_* = k_3/k_*$  and  $v_* = k_2/k_*$ , where  $k_* = (4k_1 - k_2)/(4k_1(k_2 + k_3))$ . From the condition that the concentrations are positive, it follows that the nontrivial solution is physically admissible at  $4k_1 > k_2$  because all velocity constants are considered nonnegative; at  $4k_1 = k_2$  the stationary solution ( $u_*, v_*$ ) coincides with the trivial one. The nontrivial stationary solution is a stable node or a stable focus. The eigenvalues of the Jacobi matrix for the right-hand sides of system (1) calculated at  $u = v = 0$  are equal to  $-k_3$  and  $4k_1 - k_2$  and, therefore, under the emergence of a physically admissible nontrivial solution ( $u_*, v_*$ ), the trivial solution of system (1) becomes unstable (a saddle).

Adding the diffusion terms to Eqs. (1), yields a system of partial differential equations of the reaction-diffusion type, which in the two-dimensional spatial case will be written in the form

$$\begin{cases} \partial u / \partial t = f_1 + D_1 (\partial^2 u / \partial x^2 + \partial^2 u / \partial y^2), \\ \partial v / \partial t = f_2 + D_2 (\partial^2 v / \partial x^2 + \partial^2 v / \partial y^2). \end{cases} \quad (2)$$

Here  $x$  and  $y$  are the spatial variables,  $D_1$  and  $D_2$  are the diffusion coefficients. To the best of our knowledge, system (2) does not have solutions in the form of traveling pulses or spiral waves for any values of the parameters. The characteristic features of an excitable medium can be observed if we construct zero wedges on the phase plane for the right-hand sides of the ODEs (1) and consider the trajectories of the system for different initial data. The zero wedges in the considered problem are straight lines that are not typical of an excitable medium.

Note that the classical two-component deterministic models of excitable media, such as the FitzHugh–Nagumo model, are characterized by cubic nonlinearity. In our case, the nonlinearity is quadratic and is only contained in the first equation. In addition, in the microscopic model, an excitable state is a trivial stationary state of the form ( $u = 0, v = 0$ ) and the solitary traveling pulse moves against the background of cells in the quiescent state. Such a solution appears at  $k_1 > k_2 \gg k_3$ , that is, for such parameter values when the state ( $u = 0, v = 0$ ) is an unstable stationary solution (saddle) for Eqs. (1) and (2). Thus, in this problem, a qualitative discrepancy is observed between the dynamic behavior of the models of the micro- and macrolevels. The deterministic model (2) does not represent an excitable medium.

It should be noted that the model of reactions (R1)–(R3) does not contain the diffusion process in the explicit form. The excitation is transferred from one cell to the neighboring one by a nonlocal (two-node)

reaction (R1). In a real physical system, the process of transferring excitation can occur through various physical and chemical processes, including the process of molecular diffusion.

## 6. CONCLUSIONS

The considered calculation results are primarily of fundamental interest. It appears that the stochastic model of reactions (R1)–(R3) is the simplest lattice model of an excitable medium, which can be studied using the model of the master equation and KMC simulation. Therefore, it is important to determine the basic properties of the space-time structures for this model, which has first been done in this paper. The KMC calculations show that the space-time structures in the lattice model have the basic properties of an excitable medium, which have become well known due to the investigation of the reaction-diffusion equations. However, the stochastic nature of the events on the lattice has also led to the emergence of new properties. They include the spontaneous destruction of large spiral waves and the gradual emergence of spiral turbulence. In this case, at first spiral waves are generated but then they begin to break down. For the same values of the parameters, the planar solitary waves are stable structures and no discontinuities of their leading edges are observed. It is also interesting to note that the reaction model (R1)–(R3) does not contain the diffusion process in the explicit form, which leads to a fundamental difference between the model and systems of the reaction-diffusion type.

The KMC calculation algorithm makes it possible to perform calculations on a lattice with a very large number of cells. In this respect, the following should be noted. The size of the myocardial cells (cardiomyocytes) is approximately  $20 \times 100 \mu\text{m}$  in a two-dimensional projection. Therefore, for simulating excitation waves in the heart with the help of a two-dimensional lattice model, the consideration could be confined to a small lattice ( $10^6$  cells at most) if it is assumed that each cell corresponds to one cardiomyocyte. However, the excitation waves are also observed at the subcellular level. A more detailed level of the system consideration would require a larger lattice. It is known that cardiomyocytes contain various organelles, for example, mitochondria, which are called the *energy generator* of a living cell. One cardiomyocyte contains up to  $10^4$  mitochondria, and a confocal microscope makes it possible to see an almost regular crystal-like structure made up of mitochondria [17]. In addition, it is possible to identify the so-called calcium release units (CRUs) [18]; their estimated number ranges from  $10^4$  to  $5 \times 10^4$  in one cardiomyocyte [15, 18]. Cardiomyocytes have a large number of gap junctions for interaction with neighboring cells; thus, the structure of the myocardium can be approximately represented as a three-dimensional lattice made up of mitochondria or CRUs. The study of such a system using the lattice model even in a two-dimensional approximation would require a very large lattice ( $>10^9$  cells). The algorithms and programs developed by us can be used to simulate the transfer of excitation in the cardiac muscle at both the cellular and subcellular levels, which opens up wide-ranging prospects for further research.

## REFERENCES

1. N. Wiener and A. Rosenblueth, "The mathematical formulation of the problem of conduction of impulses in a network of connected excitable elements, specifically in cardiac muscle," *Arch. Inst. Cardiol. Mexico* **16**, 205–265 (1946).
2. V. A. Vasilev, Yu. M. Romanovskii, and V. G. Iakhno, *Autowave Processes* (Nauka, Moscow, 1987) [in Russian].
3. A. Iu. Loskutov and A. S. Mikhailov, *Introduction to Synergetics, The Guide* (Nauka, Moscow, 1990) [in Russian].
4. J. D. Murray, *Mathematical Biology: I. An Introduction* (Springer, New York, 2002); *Mathematical Biology: II. Spatial Models and Biomedical Applications* (Springer, Berlin, Heidelberg, 2003).
5. J. M. Greenberg and S. P. Hastings, "Spatial patterns for discrete models of diffusion in excitable media," *SIAM J. Appl. Math.* **34**, 515–523 (1978).
6. A. B. Bortz, M. H. Kalos, and J. L. Lebowitz, "A new algorithm for Monte Carlo simulation of Ising spin systems," *J. Comp. Phys.* **17**, 10–18 (1975).
7. D. T. Gillespie, "A general method for numerically simulating the stochastic time evolution of coupled chemical reactions," *J. Comp. Phys.* **22**, 403–434 (1976).
8. De D. R. Souza, and T. Tome, "Stochastic lattice gas model describing the dynamics of the SIRS epidemic process," *Physica A* **389**, 1142–1150 (2010).
9. T. P. Shulze, "Kinetic Monte Carlo simulations with minimal searching," *Phys. Rev. E* **65**, 036704 (2002).
10. A. Chatterjee and D. G. Vlachos, "An overview of spatial microscopic and accelerated kinetic Monte Carlo methods," *J. Comput.-Aided Mater. Des.* **14**, 253–308 (2007).

11. M. Bar and M. Eiswirth, "Turbulence due to spiral breakup in a continuous excitable medium," *Phys. Rev. E* **48**, R1635–R1637 (1993).
12. A. T. Winfree, "Electrical turbulence in three-dimensional heart muscle," *Science* **266**, 1003–1006 (1994).
13. F. H. Fenton, E. M. Cherry, H. M. Hastings, and S. J. Evans, "Multiple mechanisms of spiral wave breakup in a model of cardiac electrical activity," *Chaos* **12**, 852–892 (2002).
14. J. Garcia-Ojalvo and L. Schimansky-Geier, "Noise-induced spiral dynamics in excitable media," *Europhys. Lett.* **47**, 298–303 (1999).
15. Z. Qu, G. Hu, A. Garfinkel, and J. N. Weiss, "Nonlinear and stochastic dynamics in the heart," *Phys. Rep.* **543**, 61–162 (2014).
16. A. G. Makeev, E. S. Kurkina, and I. G. Kevrekidis, "Kinetic Monte Carlo simulations of travelling pulses and spiral waves in the lattice Lotka-Volterra model," *Chaos* **22**, 023141–1–12 (2012).
17. M. Vendelin, N. Beraud, K. Guerrero, T. Andrienko, A. V. Kuznetsov, J. Olivares, L. Kay, and V. A. Saks, "Mitochondrial regular arrangement in muscle cells: a 'crystal-like' pattern," *Am. J. Physiol. - Cell Physiol.* **288**, C757–C767 (2005).
18. H. Cheng and W. J. Lederer, "Calcium sparks," *Physiol. Rev.* **88**, 1491–1545 (2008).

*Translated by I. Pertsovskaya*

SPELL: 1. OK